Relationships between hyperspectral data and components of vegetation biomass in Low Arctic tundra communities at Ivotuk, Alaska

2017 Environ. Res. Lett. 12 025003

(http://iopscience.iop.org/1748-9326/12/2/025003)

Environmental Research Letters

LETTER

Relationships between hyperspectral data and components of vegetation biomass in Low Arctic tundra communities at Ivotuk, Alaska

Sara Bratsch[1], Howard Epstein[1,5], Marcel Buchhorn[2,3,4], Donald Walker[2] and Heather Landes[1]

[1] Department of Environmental Sciences, University of Virginia, Charlottesville, VA 22904, United States of America
[2] Alaska Geobotany Center, Institute of Arctic Biology, University of Alaska Fairbanks, Fairbanks, AK 99775, United States of America
[3] Hyperspectral Imaging Laboratory, Geophysical Institute, University of Alaska Fairbanks, 903 Koyukuk Dr., Fairbanks, AK 99775, United States of America
[4] Flemish Institute for Technological Research (VITO), Boeretang 200, B-2400 Mol, Belgium
[5] Author to whom any correspondence should be addressed.

E-mail: hee2b@virginia.edu

Keywords: arctic transitions in the land-atmosphere system (ATLAS), north american arctic transect (NAAT), spectroscopy, vegetation biomass, tundra vegetation communities

OPEN ACCESS

RECEIVED
31 May 2016

REVISED
30 November 2016

ACCEPTED FOR PUBLICATION
6 January 2017

PUBLISHED
25 January 2017

Abstract

Warming in the Arctic has resulted in a lengthening of the growing season and changes to the distribution and composition of tundra vegetation including increased biomass quantities in the Low Arctic. Biomass has commonly been estimated using broad-band greenness indices such as NDVI; however, vegetation changes in the Arctic are occurring at spatial scales within a few meters. The aim of this paper is to assess the ability of hyperspectral remote sensing data to estimate biomass quantities among different plant tissue type categories at the North Slope site of Ivotuk, Alaska. Hand-held hyperspectral data and harvested biomass measurements were collected during the 1999 growing season. A subset of the data was used as a training set, and was regressed against the hyperspectral bands using LASSO. LASSO is a modification of SPLS and is a variable selection technique that is useful in studies with high collinearity among predictor variables such as hyperspectral remote sensing. The resulting equations were then used to predict biomass quantities for the remaining Ivotuk data. The majority of significant biomass-spectra relationships (65%) were for shrubs categories during all times of the growing season and bands in the blue, green, and red edge wavelength regions of the spectrum. The ability to identify unique biomass-spectra relationships per community is decreased at the height of the growing season when shrubs obscure lower-lying vegetation such as mosses. The results of this study support previous research arguing that shrubs are dominant controls over spectral reflectance in Low Arctic communities and that this dominance results in an increased ability to estimate shrub component biomass over other plant functional types.

1. Introduction

The Arctic has warmed at a greater rate than the rest of the globe through a process known as polar amplification (Serreze and Francis 2006, Walker *et al* 2012, Winton 2006). Global change in temperature from 1981–2012 is estimated to be 0.17 °C per decade (Hansen *et al* 2010), while warming in the Arctic (>66°N) has been approximately 0.60 ± 0.07 °C per decade (Comiso and Hall 2014) over the past century. Remotely sensed land surface temperature (LST) data from 1982–2008 indicate warming to be greater in the North American Arctic (+30%) than in the Eurasian Arctic (+16%) based on the Summer Warmth Index (SWI), which is the sum of average monthly surface temperatures above freezing (Bhatt *et al* 2010). Temperature increases have had probable effects on tundra ecosystems, such as a lengthening of the growing season (Huemmrich *et al* 2010, Zeng *et al* 2011), and associated increases in vegetation biomass, with Alaskan arctic tundra biomass increasing an average of 7.8% since the early 1980s (Epstein *et al* 2012).

Vascular and non-vascular (i.e. mosses and lichens) vegetation may respond differently to climate change (Huemmrich *et al* 2013). Mosses and lichens are often abundant in tundra ecosystems, though warming trends have led to atypical increases in vascular plant cover (Huemmrich *et al* 2013) and decreases in non-vascular cover (Walker *et al* 2006). This trend is not evident in all regions of the Arctic, and the High Arctic and alpine tundra have not experienced the same increases in vascular plant coverage (Cornelissen *et al* 2001). The observed increases in shrub abundance throughout the Low Arctic tundra (Myers-Smith *et al* 2011) may be due to their ability to outcompete other vegetation types, potentially through shading of non-vascular species (Chapin *et al* 1995, Cornelissen *et al* 2001, Sturm *et al* 2001).

Remote sensing has allowed scientists to monitor changes occurring in arctic vegetation at a variety of spatial and temporal scales (Stow *et al* 2004). Past studies have mapped changes in vegetation using aerial photography (Sturm *et al* 2005), coarse-scale satellite imagery such as that from the Advanced Very High Resolution Radiometer (AVHRR) (Walker 1999), and moderate-scale satellite imagery such as that from Landsat platforms (Muller *et al* 1999, Silapaswan *et al* 2001). Though vegetation change in the Arctic occurs on fine spatial scales with changes occurring at the species level, the use of high-resolution and hyperspectral imagery remains scarce (however, see Buchhorn *et al* 2013, Forbes *et al* 2010, Huemmrich *et al* 2013). Hyperspectral remote sensing allows for the use of information contained in more refined regions of the spectrum that might be obscured with broad-band data. This may be useful for identifying otherwise unobservable differences in vegetation structure and biochemical composition among plant tissue types in the Arctic.

Past studies have developed estimates of arctic tundra biomass using relationships with environmental factors (including other vegetation variables), such as SWI, gross primary productivity (GPP), and leaf area index (LAI) using simple regression (Epstein *et al* 2008, Riedel *et al* 2005a, 2005b, van der Wal and Stien 2014, Walker *et al* 2012) and multiple regression analyses (Ueyama *et al* 2013). Multiple studies have developed relationships between arctic tundra biomass and the remotely sensed broad-band Normalized Difference Vegetation Index (NDVI)—(e.g. Hope *et al* 1993, Raynolds *et al* 2012, Riedel *et al* 2005b, Stow *et al* 2004, Walker 2003). Shrubs contribute substantially to NDVI in the most southern areas of the arctic tundra, whereas bryophytes contribute relatively more to NDVI in the more northern subzones, where shrub cover is sparse (Raynolds *et al* 2012). Shrubs may become a more important component of tundra plant community biomass, as their cover and abundance increase with warmer temperatures (Riedel *et al* 2005b, Walker *et al* 1995).

Establishing relationships between plant tissue type biomass and hyperspectral information may be useful for tracking changes in arctic biomass occurring with increasing temperatures. Different regions of the visible and near infrared spectra can be used to identify functional and structural properties of vegetation communities and individual plant tissue types (Curran 1989, Ustin and Gamon 2010). Hyperspectral remote sensing (also known as imaging spectroscopy) has been useful in differentiating among vascular and non-vascular vegetation (Huemmrich *et al* 2013) and functionally distinct vegetation types in the Arctic (Buchhorn *et al* 2013). Moss and vascular plant spectra have similar reflectances in the green and near infrared (NIR) wavelength regions, whereas lichens have higher reflectance in the visible, and greater variability in species-specific reflectances (Huemmrich *et al* 2013). Dead biomass in the Arctic also influences the reflectivity spectra, particularly as shrubs begin to dominate these systems, and their leaf litter covers more low-lying plants (DeMarco *et al* 2014, Xu *et al* 2014).

Narrow-band NDVI combinations as well as other hyperspectral two-band vegetation indices (HTBVI) based on normalized difference between the bands have been used to describe biomass-spectra relationships, and show slightly better correlations with biomass than broad-band NDVI measurements (Buchhorn *et al* 2013). However, to date, hyperspectral data have not been evaluated for their utility in improving remotely sensed estimates of tundra biomass. The goal of this research was therefore to establish relationships between tundra biomass components and hyperspectral data from a Low Arctic site in Alaska using handheld hyperspectral remote sensing. Our specific objective is to develop relationships between a hierarchy of tundra vegetation biomass components (i.e. at landscape, plant community, plant functional type, and tissue type levels) and hyperspectral reflectance data. Analyses of these relationships across the various scales will inform the degree to which we can generalize relationships between tundra biomass and hyperspectral information.

2. Methods

2.1. Study area

Ivotuk, Alaska (68.49° N, 155.74° W) is located on the North Slope of the Brooks Mountain Range (Epstein *et al* 2004, Riedel *et al* 2005a, 2005b), and was one of seven sites established as part of the Arctic Transitions in the Land-Atmosphere System (ATLAS) project (McGuire 2003, Walker 2003, Walker *et al* 2003). Ivotuk is part of the Western Alaska Transect that starts in the north at Barrow and goes south through Atqasuk and Oumalik to Ivotuk (Epstein *et al* 2008, Jia *et al* 2002, McGuire 2003, Walker 2003).

Ivotuk is located in bioclimatic subzone E, which includes the Arctic Foothills and non-forested areas of the Seward Peninsula (Walker *et al* 2003). The

Table 1. Biomass sampling dates and observation count per vegetation community during the 1999 growing season, where *n* is the number of observations.

Growing season	MAT	MNT	MT	ST
Early	5 June–3 July (n = 22)	8 June–10 July (n = 20)	10 June–9 July (n = 20)	6 June–11 July (n = 20)
Peak	13 July–14 August (n = 28)	25 July–22 August (n = 33)	16 July–24 August (n =24)	26 July–23 August (n = 20)

Circumpolar Arctic Vegetation Map (CAVM) identifies five bioclimatic subzones (A-E) based on differences in climate, vegetation, topography, substrate biogeochemistry, and NDVI (CAVM 2003, Raynolds *et al* 2006, Walker *et al* 2005). Subzone E is the southernmost and warmest of the five tundra subzones. Ivotuk is largely a tussock tundra ecosystem also dominated by deciduous shrubs (Walker 2003). It is located at an elevation of approximately 550m (Epstein *et al* 2004). From 1991–2001 (a time period that encompasses the sampling that will be used for this research), the site received an annual average of 202 mm precipitation, had a July maximum temperature of approximately 12 °C, an annual temperature of −10.9 °C, and a 110-day growing season (Jia *et al* 2002, Riedel *et al* 2005a, 2005b).

The site of Ivotuk is comprised of the four plant communities: moist acidic tundra (MAT), moist nonacidic tundra (MNT), mossy tussock tundra (MT) and shrub tundra (ST). MAT and MNT are differentiated by soil acidity, with MAT occurring on soils with pH $<$ 5.0–5.5, and MNT occurring on soils with pH $\geq$ 5.0–5.5 (Walker 2003, Walker *et al* 1994). MAT, also referred to as tussock-graminoid tundra, is dominated by dwarf erect shrub species such as *Betula nana*, and the tussock sedge *Eriophorum vaginatum* (Walker *et al* 1994). *Betula nana* is absent in MNT due to low soil acidity. Mosses, graminoids, non-tussock sedges, and prostrate dwarf shrubs such as *Dryas integrifolia* dominate in MNT communities (Jia *et al* 2004, Walker *et al* 1994). MT contributes greatly to biomass quantities in tundra systems, and is typified as an acidic tussock tundra with abundant *Sphagnum* mosses (Tenhunen *et al* 1992). ST is dominated by shrubs such as *Salix alaxensis, Betula nana,* and *Alnus crispa* (Muller *et al* 1999), and is interspersed with graminoids, forbs, lichens, and mosses.

2.2. Data collection and processing

One 100 m × 100 m grid was established in each of the four vegetation communities (Epstein *et al* 2008, Riedel *et al* 2005a, 2005b, Walker 2003, Walker *et al* 2003). Spectroscopy data were collected during the 1999 growing season at biweekly intervals from 5 June–26 August and grouped according to early and peak growing season (table 1). Spectral measurements were made using an Analytical Spectral Devices FieldSpec spectro-radiometer with a spectral resolution of 1.42 nm and a spectral range of 330.79–1061.78 nm (Riedel *et al* 2005a, 2005b). Spectral measurements were collected from ten random grid points established in each of the four vegetation grids. The same 10 points were used for spectral data collection for the duration of the growing season. Biomass data were collected biweekly from ten 20 × 50 cm plots adjacent to these spectral gridpoints (Epstein *et al* 2004, 2008, Riedel *et al* 2005a, 2005b, Walker 2003). Both biomass and spectral measurements were collected from an additional ten gridpoints for one collection week during peak growing season (Riedel *et al* 2005a, 2005b).

Vascular plants were clipped at the top of the moss surface, and mosses were clipped at the base of the green layer (Epstein *et al* 2004, Riedel *et al* 2005a, 2005b, Walker 2003). Biomass samples were sorted into seven functional categories including evergreen and deciduous shrubs, graminoids, horsetails, other forbs (hereafter simply 'forbs'), bryophytes, and lichens (Riedel *et al* 2005a, 2005b, Walker 2003). Samples were oven-dried at 55 °C for 48 h before being taken back to the University of Virginia for further processing (Epstein *et al* 2004). Graminoids were divided into live and dead materials (Riedel *et al* 2005a, 2005b). Evergreen and deciduous shrubs were divided into woody, foliar live, and foliar dead materials (Epstein *et al* 2004, Riedel *et al* 2005a, 2005b).

2.3. Species composition

Species data were collected using the Braun-Blanquet method (Westhoff and van der Meel 1973). Mosses were one of the most abundant plant functional types in all four communities (table 2). *Hylocomium splendens* (51%–75%) was the most common in MAT and ST, where the deciduous shrub *Rubus chamaemorus* also dominates species composition (51%–75%). The moss *Tomentypnum nitens,* the evergreen shrub *Dryas integrifolia*, and the graminoid *Carex bigelowii* all occurred with a frequency of (26%–50%) in MNT. Graminoids were the most abundant PFT in MT, with the largest contributor as the species *Eriophorum vaginatum* (51%–75%).

2.4. Spectral processing

Original field spectroscopy data from Ivotuk were resampled to 5 nm wide hyperspectral narrowbands (HNBs) ranging from 400–1000 nm. Aggregating to 5 nm bands increases the signal-to-noise ratio (SNR), reduces wavelength redundancy issues, and potentially makes results more transferable to other sites and data that may have been collected with different

Table 2. Dominant plant species at Ivotuk, Alaska per plant vegetation community and plant functional type. Species are presented along with their Braun-Blanquet percentages. Most abundant species are shown in gray.

Plant Functional Type	Vegetation Community			
	MAT	MNT	MT	ST
Deciduous shrub	*Betula nana* ssp. *exilis* (26%–50%)	*Salix reticulata* (6%–25%)	*Rubus chamaemorus* (6%–25%)	*Rubus chamaemorus* (51%–75%)
Evergreen shrub	*Rhododendron tomentosum* subsp. *decumbens* (26%–50%)	*Dryas integrifolia* (26%–50%)	*Rhododendron tomentosum* subsp. *decumbens* (6%–25%)	*Pyrola grandiflora* (1%–5%)
Forb	*Petasites frigidus* (6%–25%)	*Geum glaciale* (6%–25%)	—	*Petasites frigidus* (26%–50%)
Graminoid	*Eriophorum vaginatum* (26%–50%)	*Carex bigelowii* (26%–50%)	*Eriophorum vaginatum* (51%–75%)	*Eriophorum angustifolia* (26%–50%)
Lichen	*Baeomyces carneus*, and *Peltigera aphthosa* (1%–5%)	*Thamnolia vermicularis* s. *subuliformis* (6%–25%)	*Cladonia amaurocraea*, *C. arbuscula*, *C. stygia*, *Dactylina arctica*, *Flavocetraria cucullata*, *Peltigera rufescens*, and *Thamnolia vermicularis* var. *subuliformis* (0.5%)	*Peltigera leucophlebia* (1%–5%)
Moss	*Hylocomium splendens* (51%–75%)	*Tomentypnum nitens* (26%–50%)	*Sphagnum lenense* (26%–50%)	*Hylocomium splendens* (51%–75%)

instruments. As a quality assurance step, reflectance spectra from Ivotuk were examined visually for irregularities. Irregular spectra were removed before analysis in an effort to overcome the heterogeneous nature of vegetation at Ivotuk and develop a more diagnostic spectral signature.

2.5. Data analysis

Regularization methods such as the least absolute shrinkage and selection operator (LASSO) are valuable tools for addressing many of the analytical problems affecting hyperspectral remote sensing such as high collinearity. LASSO is a modified form of partial least squares regression that reduces model complexity using a regularization parameter and is unaffected by the order of variable entry into a model (Tibshirani 1996). The regularization parameter works by shrinking variable coefficients toward zero, and eliminating variables from the model when their coefficients reach zero. As such, LASSO is an effective variable selection and dimensionality reduction technique.

Data were first analyzed without separation by vegetation community, meaning that all biomass data from either early or peak season was used for analysis. This was then repeated with separation by MAT, MNT, MT, or ST community in order to establish relationships between biomass categories and spectral variables specific to a vegetation community. Sample size per vegetation community ranged from 20–22 during early growing season and from 20–33 during peak growing season (table 1). A simple random sample of one-half of the Ivotuk data was used to create the training set. The remaining one-half was used to create the test set. Plant tissue type biomass quantities were then regressed against spectra using LASSO regression from the 'glmnet' package in R (Friedman *et al* 2010).

3. Results

3.1. Total vegetation biomass

3.1.1. *Biomass quantities.*

Total biomass across all four vegetation communities during early growing season was 768.9 g m^{-2}. The greatest contributor to live biomass was moss (306.9 g m^{-2}), followed by deciduous shrub (183.6 g m^{-2}), evergreen shrub (61.9 g m^{-2}), graminoid (37.1 g m^{-2}), lichen (22.2 g m^{-2}), and forb (8.7 g m^{-2}) (figure 1).

Total biomass for all four vegetation communities during peak growing season was 851.2 g m^{-2}. The greatest contributor to live biomass was moss (333.2 g m^{-2}), followed by deciduous shrubs (155.0 g m^{-2}), evergreen shrubs (89.0 g m^{-2}), graminoid (58.8 g m^{-2}), lichen (32.2 g m^{-2}), and forb (10.8 g m^{-2}) (figure 2).

3.1.2. *Optimal HNBs.*

The majority of hyperspectral narrow bands (HNBs) present in the biomass-spectra relationships for early growing season and without separation by community type were in the NIR wavelength region (725–1 000 nm) (figure 3). The next most common wavelength region was the blue (450–495 nm) followed by the NIR and green (495–570 nm), the red edge (680–725 nm) and yellow (570–590 nm). The least common wavelength region was red (620–680). No relationships used bands in the orange wavelength region (590–620 nm) of

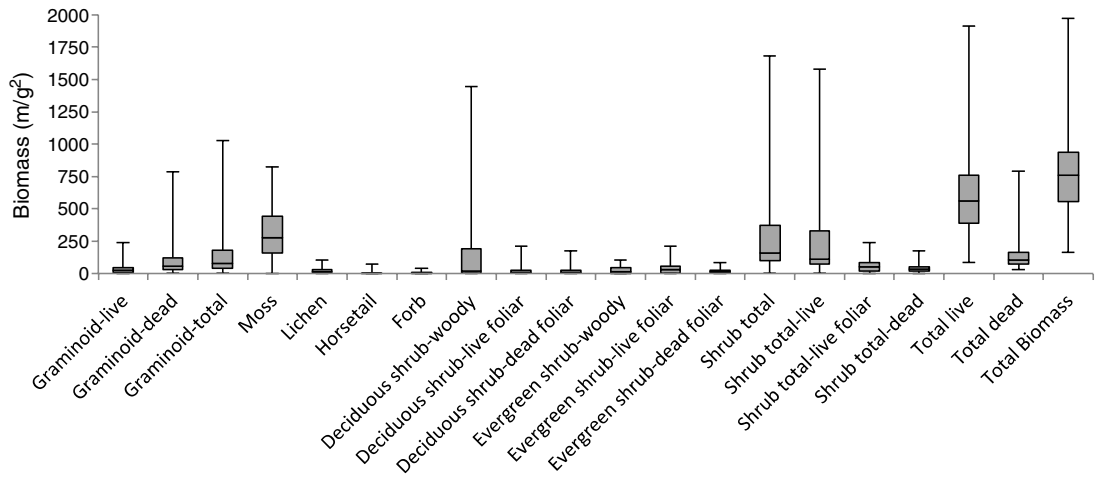

Figure 1. Boxplot of biomass quantities per plant tissue type during early growing season at Ivotuk, Alaska without separation by vegetation community.

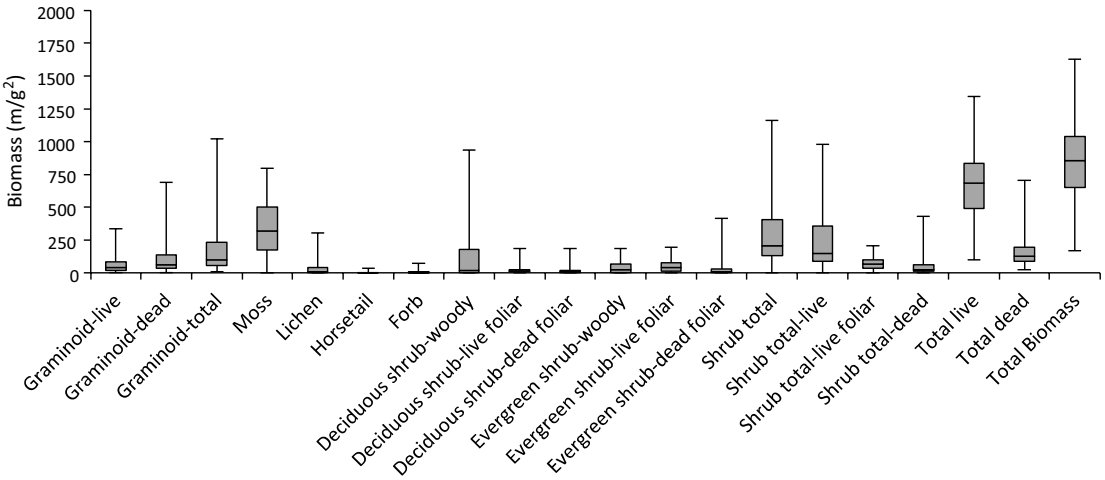

Figure 2. Boxplot of biomass quantity per plant tissue type biomass component during peak growing season at Ivotuk, Alaska.

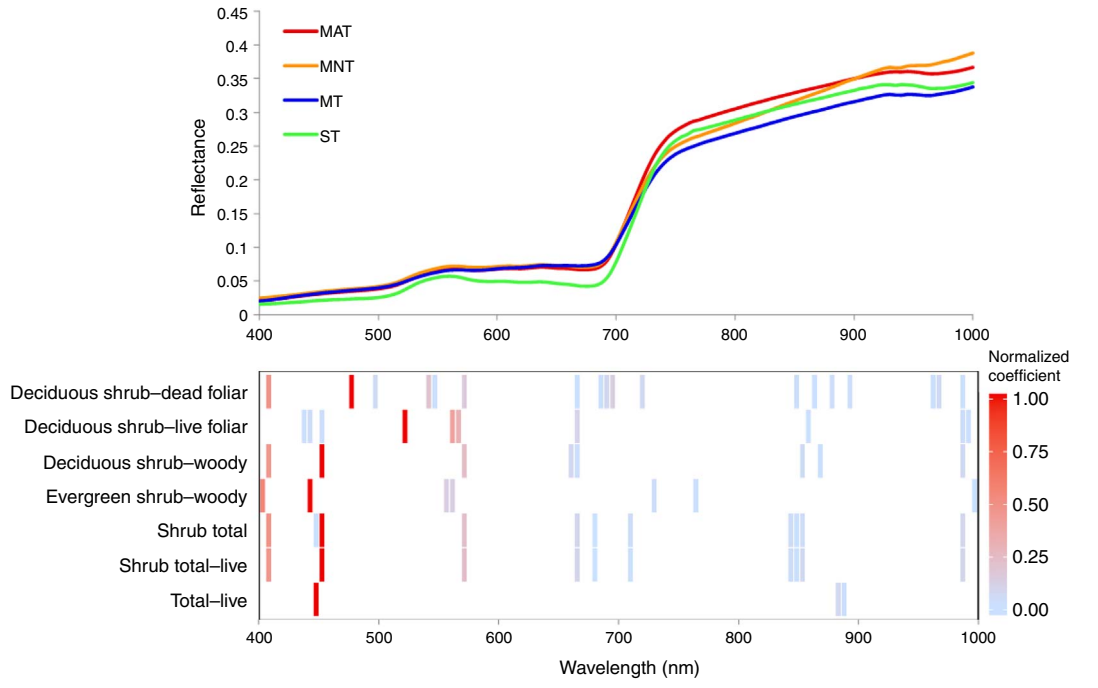

Figure 3. Mean reflectance for all vegetation communities during early growing season along with the normalized coefficients for the optimal HNBs associated with the plant tissue type categories for total biomass.

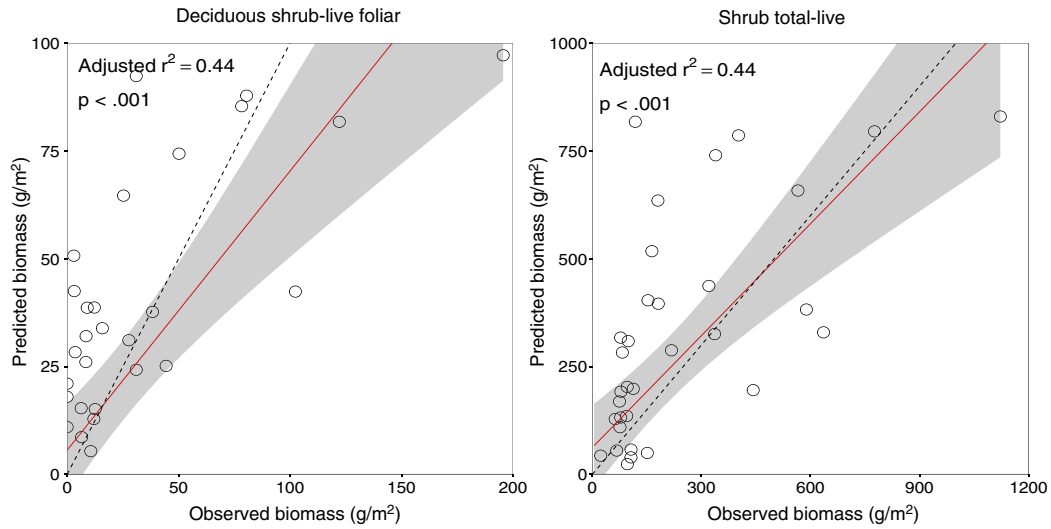

Figure 4. Best fit relationships between plant tissue type biomass components during early growing season without separation by vegetation community. The best-fit line is shown in red along with 95% confidence intervals shaded in gray. The dashed line is the 1:1 line.

Table 3. Significant relationships during early growing season without separation by vegetation community.

Plant Tissue Type	Predictor Bands	Adjusted *r*-square	*p*
Deciduous shrub-live foliar	435, 440, 450, 520, 560, 565, 665, 860, 990, 995	0.44	<.001
Shrub total-live	405, 450, 570, 665, 680, 710, 845, 850, 855, 990	0.44	<.001
Evergreen shrub-woody	400, 440, 555, 560, 730, 765, 1000	0.43	<.001
Deciduous shrub-woody	405, 450, 570, 660, 665, 855, 870, 990	0.40	<.001
Shrub total	405, 445, 450, 570, 665, 680, 710, 845, 850, 855, 990	0.39	<.001
Deciduous shrub-dead foliar	405, 475, 495, 540, 545, 570, 665, 685, 690, 695, 720, 850, 865, 880, 895, 965, 970, 990	0.33	<.001
Total-live	445, 885, 890	0.31	<.001

the spectrum. While the majority of HNBs used in significant biomass-spectra relationships were located in the NIR, those in the blue and green wavelength regions load more highly, and therefore more significantly affect the biomass-spectra relationships. Those in the yellow, orange, and red also load more highly than those in the NIR. The best relationships between plant tissue type and spectral reflectances were for deciduous shrub-live foliar and shrub total-live (adjusted $r^2 = 0.44$) (figure 4, table 3).

The majority of HNBs present in the biomass-spectra relationships for peak growing season and without separation by community type were in the near infrared wavelength and green wavelength regions (figure 5). The next most common was the red edge, followed by the NIR, blue and red, and finally orange wavelength region. In addition to being one of the dominant spectral regions, green wavelengths load more highly than most other segments. Blue also loads very highly, but is not one of the most common spectral regions in these relationships. Bands in the yellow, orange, red, and lower wavelengths of the NIR also load more highly than longer wavelengths. The best relationship during peak growing season without separation by vegetation community type was for shrub total-live (adjusted $r^2 = 0.65$) (figure 6, table 4).

3.2. Biomass with separation by vegetation community

3.2.1. *Biomass quantities.*

Shrub tundra had the greatest total biomass during early growing season (1063.3 g m^{-2}), followed by MAT (683.5 g m^{-2}), MT (679.6 g m^{-2}), and MNT (657.9 g m^{-2}) (figure 7). The plant tissue type that contributed the most biomass to MAT was graminoid-dead (173.6 g m^{-2}). Moss was the greatest contributor in both MNT (462.5 g m^{-2}) and MT (288.4 g m^{-2}). Deciduous shrub-woody was the greatest contributor in ST (542.7 g m^{-2}).

ST had the greatest total quantity of biomass during peak growing season (1129.1 g m^{-2}), followed by MAT (842.2 g m^{-2}), MT (815.2 g m^{-2}), and MNT (724.8 g m^{-2}) (figure 8). The largest plant tissue type biomass contributor was moss in all communities except ST at 201.5 g m^{-2} in MAT, 445.8 g m^{-2} in MNT, and 349.7 g m^{-2} in MT. Deciduous shrub-woody was the greatest contributor in ST at 498.3 g m^{-2}.

3.2.2. *Optimal HNBs*

The majority of HNBs for early growing season with separation by vegetation community type were located in the red edge wavelength region (figure 9). The next most common region of the spectrum was the green,

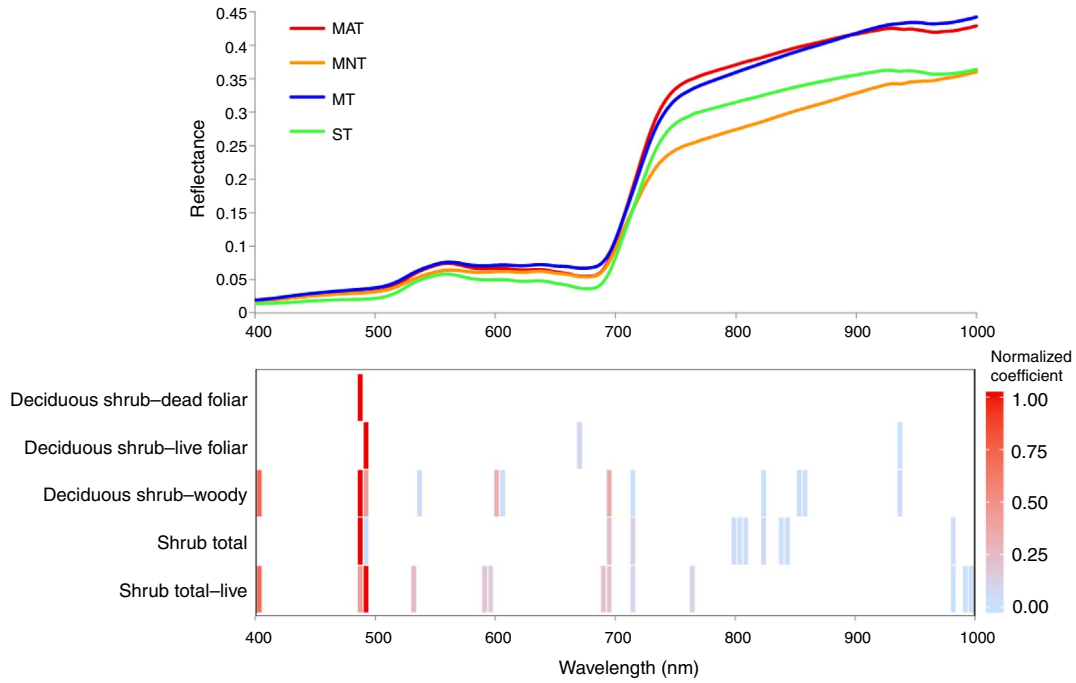

Figure 5. Mean reflectance for all vegetation communities during peak growing season along with the normalized coefficients for the optimal HNBs associated with the plant tissue type categories for total biomass.

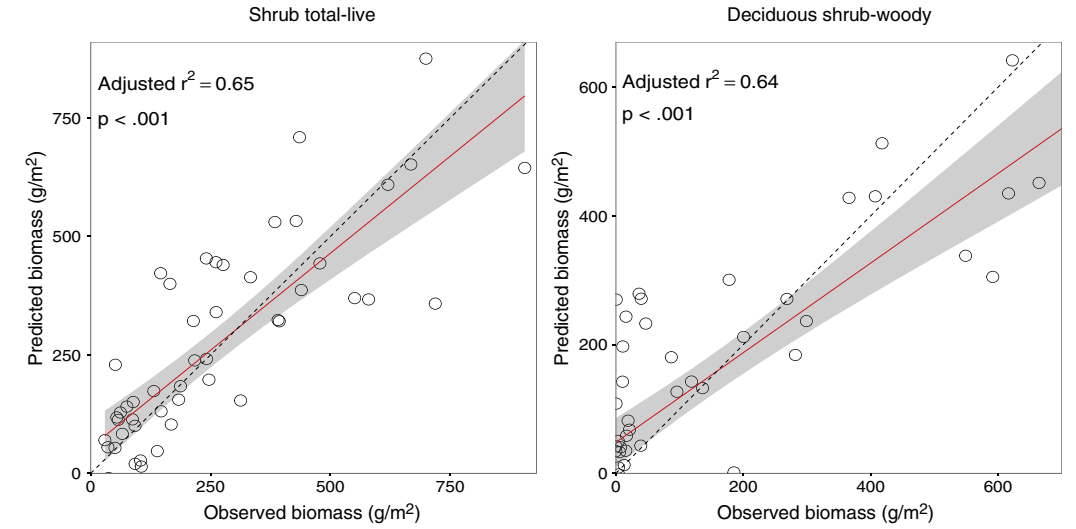

Figure 6. Best fit relationships between plant tissue type biomass components during peak growing season without separation by vegetation community. The best-fit line is shown in red along with 95% confidence intervals shaded in gray. The dashed line is the 1:1 line.

Table 4. Significant relationships for plant tissue types during peak growing season without separation by vegetation community.

Plant Tissue Type	Predictor Bands	Adjusted *r*-square	*p*
Shrub total-live	400, 485, 490, 530, 590, 595, 690,695 715, 765, 985, 995, 1000	0.65	<.001
Deciduous shrub-woody	400, 485, 490, 535, 600, 605, 695, 715, 825, 855, 860, 940	0.64	<.001
Shrub total	400, 485, 490, 695, 715, 800, 805, 810, 825, 840, 845, 985	0.63	<.001
Deciduous shrub-live foliar	490, 670, 940	0.39	<.001
Deciduous shrub-dead foliar	485	0.32	<.001

followed by red, then blue, yellow, the NIR, and orange. Bands in the red edge wavelength region were dominant in MAT and MNT, while bands in the green wavelengths were dominant in ST. Bands in the red and red edge loaded highly in MAT, with bands in the blue and green loading highly for the relationship between MAT spectra and evergreen shrub-live foliar only. Bands in the red edge and the blue loaded highly

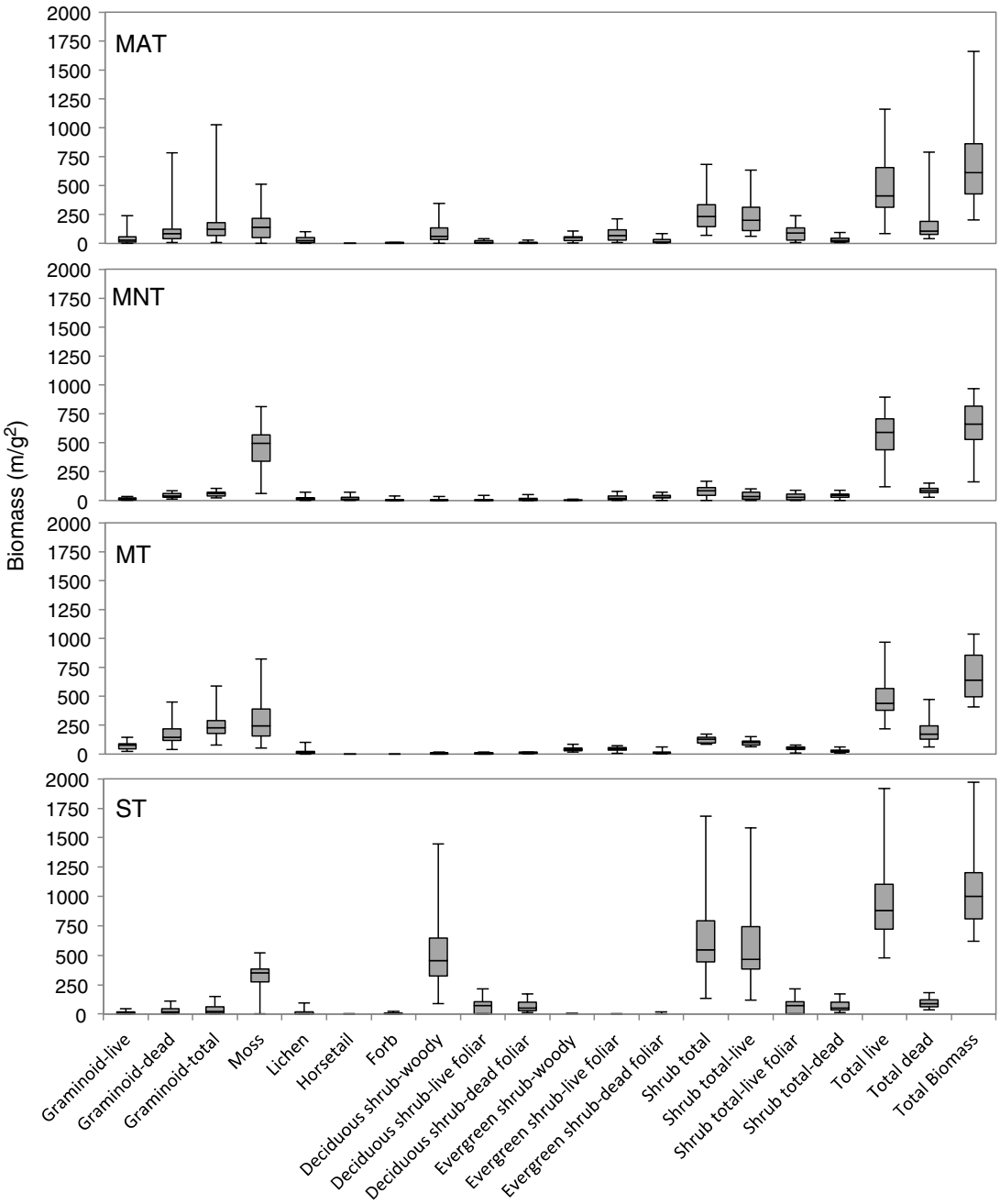

Figure 7. Boxplot of biomass quantity per plant tissue type biomass component during early growing season for vegetation communities of MAT (*a*), MNT (*b*), MT (*c*), ST (*d*) at Ivotuk, Alaska.

for MNT, and bands in the green and red loaded highly in ST. The best relationship between biomass and spectral reflectances in MAT and ST was for evergreen shrub-live foliar (figure 10, table 5). MNT had two significant relationships with shrub total-live foliar and shrub total-live (adjusted r^2 = 0.33).

The majority of HNBs for peak growing season with separation by vegetation community type were located in the red edge and blue wavelength regions (figure 11). The next most common region was the NIR, followed by yellow and green. No bands in the orange or red wavelength regions were used. Bands in the green and red edge were dominant in MNT, while bands in the red edge were dominant in MT. Bands in the blue and NIR were equally dominant in ST. Bands in the blue, red edge, and green load most highly in MNT. Bands in the blue load most highly in MT, and bands in the blue load more highly than those in the NIR in ST. MNT and ST both had significant relationships to shrub biomass tissue type, while MAT had no significant relationships, and MAT had relationships to total biomass and moss (figure 12, table 6).

4. Discussion

This study uses LASSO regression to identify relationships between biomass categories and significant wavelengths in hyperspectral ground-based data in

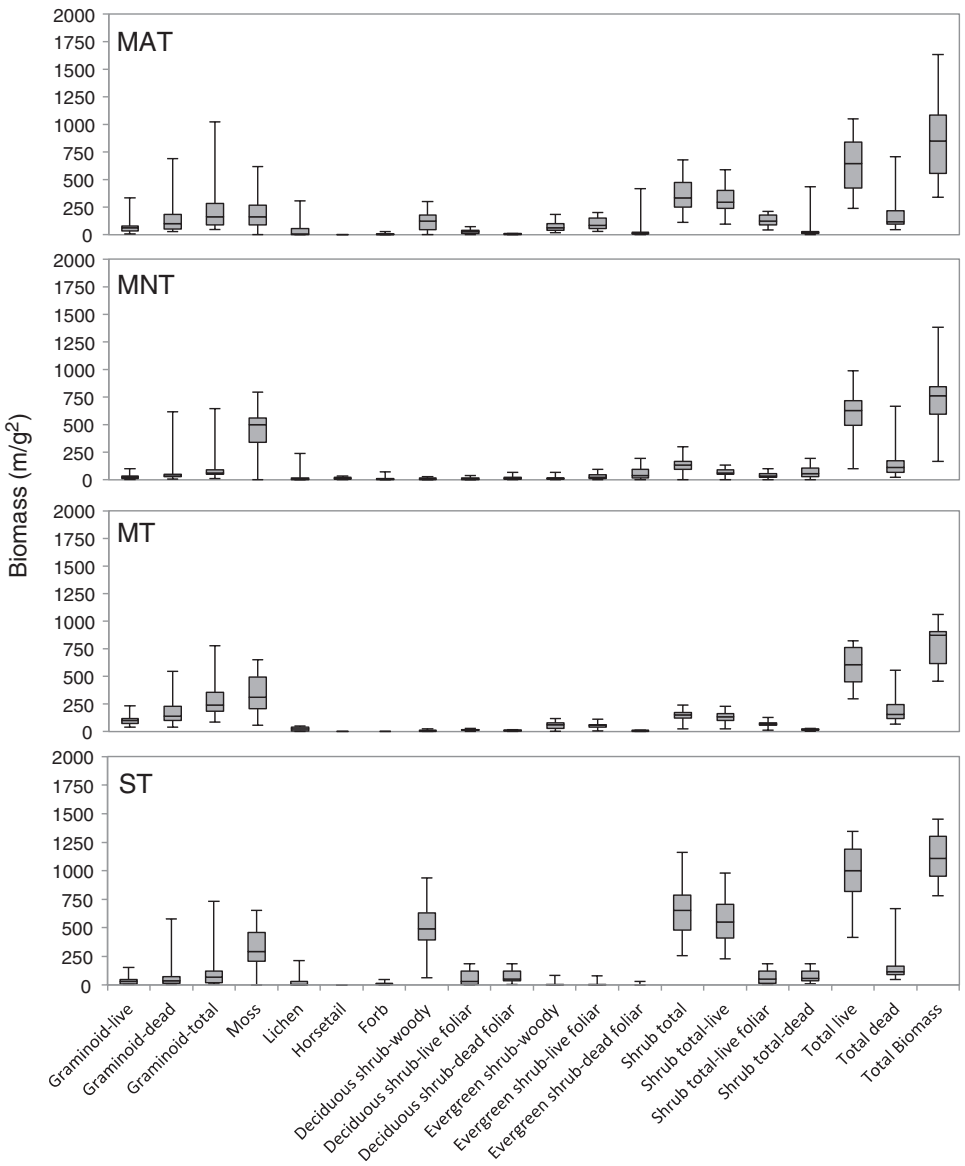

Figure 8. Boxplot of biomass quantity per plant tissue type biomass component during peak growing season for the four vegetation communities of MAT (*a*), MNT (*b*), MT (*c*), ST (*d*) at Ivotuk, Alaska.

four vegetation communities at Ivotuk, Alaska. Biomass-spectra relationships were established both with and without separation by vegetation community type. Our results support the Riedel *et al* (2005b) findings that shrubs are dominant controls over spectral reflectances at Ivotuk, as 65% of significant biomass-spectra relationships were for shrub or shrub component parts. However, our findings suggest that areas of the spectra outside the typical range of broad-band NDVI (red: 620–680 nm; NIR: 725–1 000 nm) may be more useful for creating biomass-spectra relationships as bands in the blue (450–495 nm), green (495–570 nm), and red edge (680–725 nm) wavelength regions loaded very highly for the majority of biomass-spectra relationships. These findings support results by Bratsch *et al* (2016) indicating that bands outside typical NDVI ranges may be more useful for discriminating among vegetation community types than simply NDVI itself.

While mosses contributed the greatest quantities of biomass in vegetation communities at Ivotuk Alaska, the majority of significant relationships were for shrub vegetation at all times of the growing season, an aspect potentially due to shading by overlying shrub vegetation. Past research has highlighted the importance of live foliar shrub materials as dominant controls over spectral reflectance in MAT and ST, but has noted that graminoids and bryophytes tend to dominate in MNT and MT (Riedel *et al* 2005b). This research suggests that MAT, MNT, and MT all have spectral reflectances associated with shrub biomass while the peak MT spectral signature is closely associated with moss biomass, and is the only example of significant moss-spectra relationship in this study. Therefore, although mosses comprise large quantities of vegetation biomass, we may not be able to accurately estimate this biomass component due to shading from overlying vegetation.

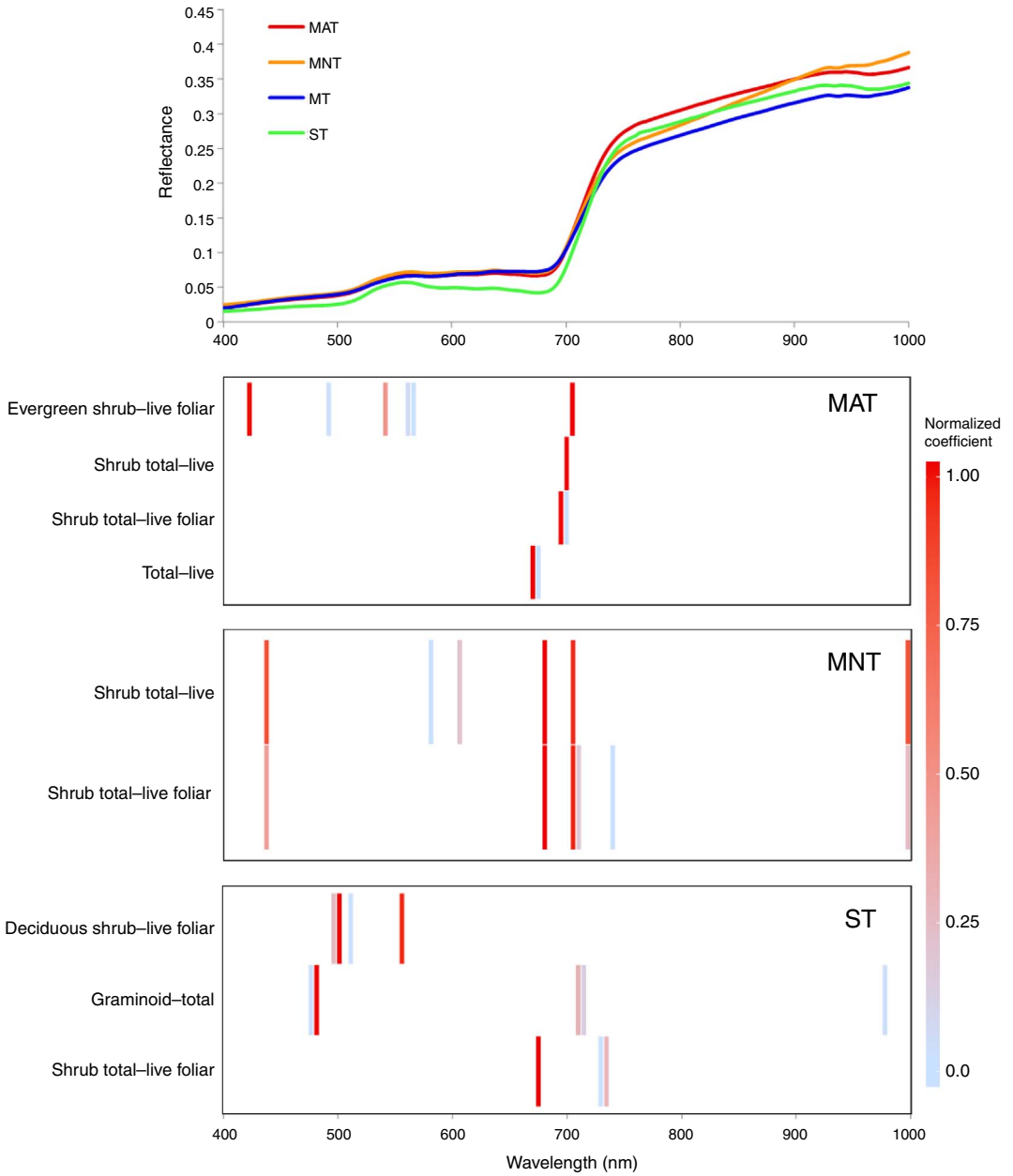

Figure 9. Mean reflectance for all vegetation communities during early growing season along with the normalized coefficients for the optimal HNBs associated with the plant tissue type categories for biomass per vegetation communities. There were no significant relationships for MT.

There were twenty-six total significant relationships between plant tissue type biomass components and spectra at Ivotuk, Alaska (see tables 3–6). Seventeen significant relationships were for shrub or shrub component parts, six were for lower-lying plant tissue types such as dead biomass, graminoid, and moss; and three were for total categories. There were sixteen significant biomass-spectra relationships during early growing season but only ten during peak growing season. Stratification of vegetation by plant community type improved the relationships between spectral reflectance values and biomass only during the early growing season. During the peak of the growing season, these relationships worked well across all four vegetation types analyzed. If the vegetation type-specific relationships were to be used, these communities can be discriminated among each other, also using hyperspectral data (Bratsch *et al* 2016).

Differences in composition of vascular and non-vascular vegetation determine many of the spectral differences among vegetation communities in the Alaskan Arctic (Huemmrich *et al* 2013). Biomass-spectra relationships per individual community are stronger during early growing season, which may be attributable to less shrub coverage, and more contribution from non-vascular plant species to spectral signatures. These results suggest that differences in biomass-spectra relationships are more apparent during early growing season, and decrease during peak growing season, resulting in a decreased ability to develop significant relationships between biomass and spectra during peak growing season at the

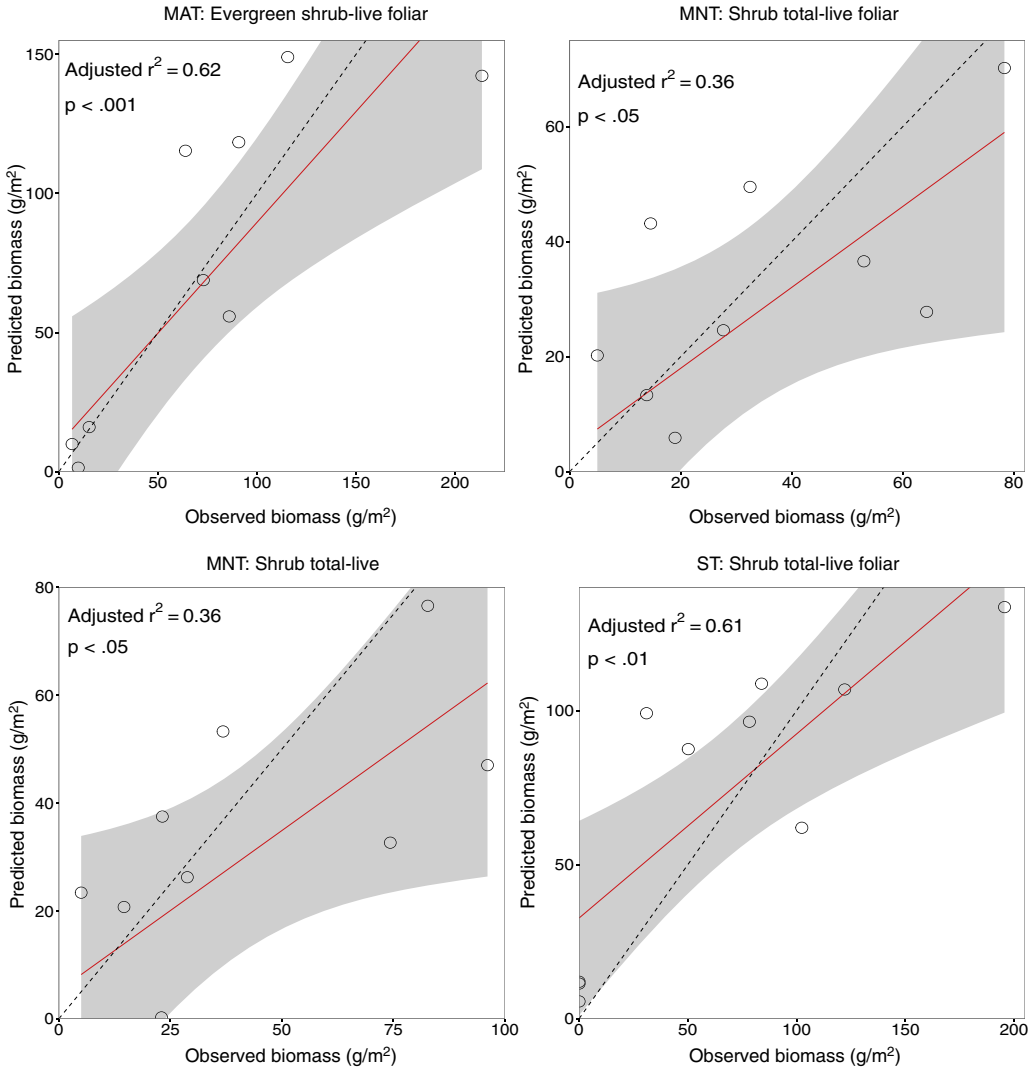

Figure 10. Best fit relationships between plant tissue type biomass components during early growing season for four vegetation communities at Ivotuk, Alaska. The best-fit line is shown in red along with 95% confidence intervals shaded in gray. The dashed line is the 1:1 line.

Table 5. Significant relationships during early growing season for four vegetation communities at Ivotuk, Alaska.

Community	Plant Tissue Type	Predictor Bands	Adjusted *r*-square	*p*
MAT	Evergreen shrub-live foliar	420, 490, 540, 560, 565, 705	0.62	<.001
MAT	Shrub total-live foliar	695, 700	0.56	<.01
MAT	Shrub total-live	700	0.33	<.05
MAT	Total-live	670, 675,	0.33	<.05
MNT	Shrub total-live foliar	435, 680, 705, 710, 740, 1000	0.36	<.05
MNT	Shrub total-live	435, 580, 605, 680, 705, 1000	0.36	<.05
ST	Shrub total-live foliar	675, 730, 735	0.61	<.01
ST	Graminoid-total	475, 480, 710, 715, 980	0.59	<.01
ST	Deciduous shrub-live foliar	495, 500, 510, 555	0.46	<.05

individual community level. The problem with establishing biomass-spectra relationships for individual communities during peak growing season may be attributable to increased shrub cover during peak growing season, shading of non-vascular vegetation, similarities in species composition, and shrubs obscuring spectral information from underlying vegetation. These results suggest that community separation may be a better method for establishing biomass-hyperspectral relationships during early growing season, while analyses without community separation may be a better method during peak growing season.

Overall, hyperspectral bands associated with pigments (400–700 nm) loaded highest when establishing biomass-spectra relationships without separation by

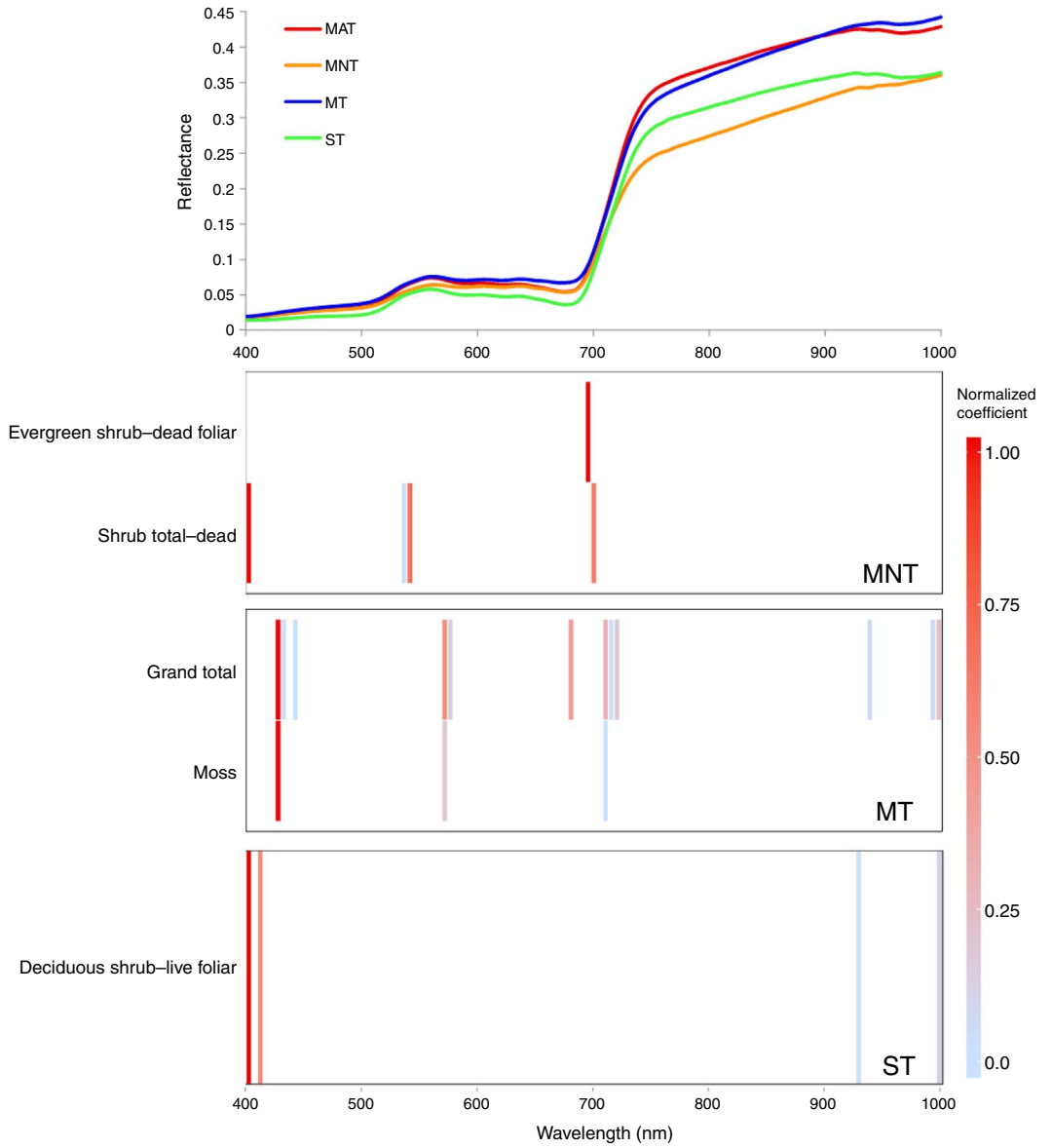

Figure 11. Mean reflectance for all vegetation communities during peak growing season along with the normalized coefficients for the optimal HNBs associated with the plant tissue type categories for biomass per vegetation communities.

vegetation community type during both early and peak growing season. Bands in the NIR that are associated with plant structure were only significant for four relationships during early growing season with separation by vegetation community type. These relationships were for live and live foliar shrub components. Unlike (Bratsch *et al* 2016) where vegetation structure becomes more important for community discrimination during peak growing season and reliance on NIR bands increases, in this study, the high loading of wavelengths in the green and blue remains consistent during all times of the growing season. This indicates a strong reliance on hyperspectral wavelengths associated with chlorophyll absorption during all parts of the growing season. Bands associated with chlorophyll in general, some of these outside the typical range of broad-band NDVI, are the most significant for determining biomass quantities at Ivotuk, Alaska.

5. Conclusion

Arctic vegetation communities vary in plant species and plant functional type composition and biomass quantities. Along with physiological features in plant species, these differences result in spectral variations that are identifiable through hyperspectral remote sensing, and allow for the creation of biomass-spectra relationships. This study presents an example of the use of hyperspectral information for establishing these biomass-spectra relationships. This allows us to create remote ways of tracking increases in biomass quantities with climate change without incurring the large monetary and time cost traditionally associated with arctic research. The above research presents a method for developing biomass-spectral relationships using handheld hyperspectral data that can then be used to identify bands on upcoming satellite missions such as the NASA Hyperspectral

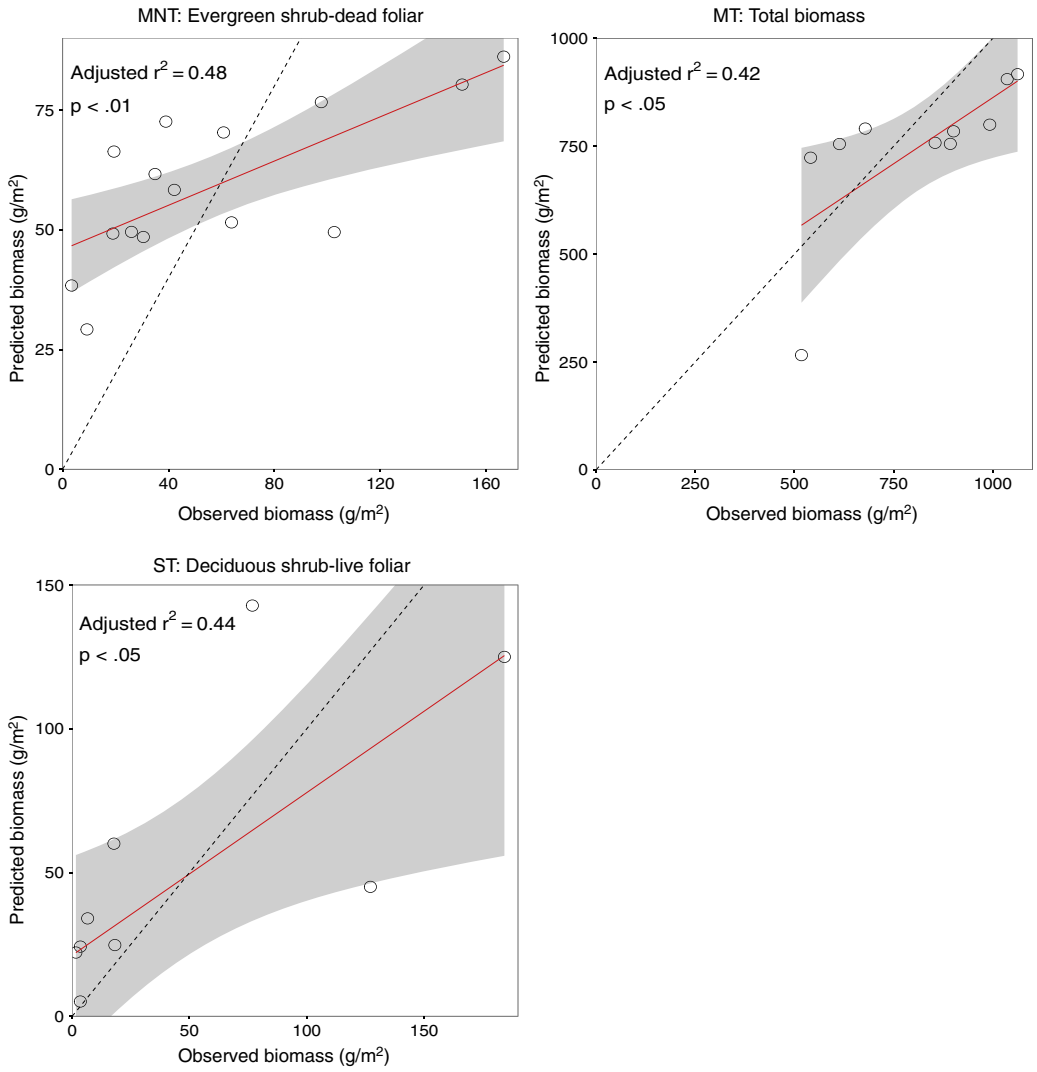

Figure 12. Best fit relationships between plant tissue type biomass components for vegetation communities during peak growing season. The best-fit line is shown in red along with 95% confidence intervals shaded in gray. The dashed line is the 1:1 line.

Table 6. Significant relationships during peak growing season for four vegetation communities at Ivotuk, Alaska.

Community	Plant Tissue Type	Predictor Bands	Adjusted *r*-square	*p*
MNT	Evergreen shrub-dead foliar	695	0.48	<.01
MNT	Shrub total-dead	400, 535, 540, 700	0.45	<.01
MT	Grand total	425, 430, 440, 570, 575, 680, 710, 715, 720, 940, 995, 1000	0.42	<.05
MT	Moss	425, 570, 710	0.36	<.05
ST	Deciduous shrub-live foliar	400, 410, 930, 1000	0.44	<.05

Infrared Imager (HyspIRI) and the German Environmental Mapping and Analysis Program (EnMAP) that would be useful for tracking changes in vegetation biomass. Establishing these relationships at the ground level allows for the potential use of these methods to monitor changes to biomass occurring with increasing temperatures in the Arctic at much larger spatial and longer temporal extents.

References

Bhatt U S *et al* 2010 Circumpolar arctic tundra vegetation change is linked to sea ice decline *Earth Interact.* **14** 1–20

Bratsch S *et al* 2016 Differentiating among four arctic tundra plant communities at Ivotuk, Alaska using field spectroscopy *Remote Sens.* **8** 51

Buchhorn M *et al* 2013 Ground-based hyperspectral characterization of Alaska tundra vegetation along environmental gradients *Remote Sens.* **5** 3971–4005

CAVM Circumpolar Arctic Vegetation Map. 2003 (1:7, 500 000 scale), Conservation of Arctic Flora and Fauna (CAFF) Map No. 1. U.S. Fish and Wildlife Service, Anchorage, Alaska

Chapin F S *et al* 1995 Responses of arctic tundra to experimental and observed changes in climate *Ecology* **76** 694–711

Comiso J C and Hall D K 2014 Climate trends in the Arctic as observed from space *Wiley Interdiscip. Rev. Clim. Change* **5** 389–409

Cornelissen J H *et al* 2001 Global change and arctic ecosystems: is lichen decline a function of increases in vascular plant biomass? *J. Ecol.* **89** 984–94
Curran P J 1989 Remote sensing of foliar chemistry *Remote Sens. Environ.* **30** 271–8
DeMarco J *et al* 2014 Effects of arctic shrub expansion on biophysical versus biogeochemical drivers of litter decomposition *Ecology.* **95** 1861–75
Epstein H E *et al* 2004 Detecting changes in arctic tundra plant communities in response to warming over decadal time scales *Glob. Change Biol.* **10** 1325–34
Epstein H E *et al* 2012 Dynamics of aboveground phytomass of the circumpolar Arctic tundra during the past three decades *Environ. Res. Lett.* **7** 015506
Epstein H E *et al* 2008 Phytomass patterns across a temperature gradient of the North American arctic tundra *J. Geophys. Res.* **113** G03S02
Forbes B C *et al* 2010 Russian Arctic warming and 'greening' are closely tracked by tundra shrub willows *Glob. Change Biol.* **16** 1542–54
Friedman J *et al* 2010 Regularization paths for generalized linear models via coordinate descent *J. Stat. Softw.* **33** 1–22
Hansen J *et al* 2010 Global surface temperature change *Rev. Geophys.* **48** RG4004
Hope A *et al* 1993 The relationship between tussock tundra spectral reflectance properties and biomass and vegetation composition *Int. J. Remote Sens.* **140** 1861–74
Huemmrich F *et al* 2013 Arctic tundra vegetation functional types based on photosynthetic physiology and optical properties *IEEE J. Selected Topics in Applied Earth Observations and Remote Sensing* **6** 265–75
Huemmrich K F *et al* 2010 Tundra carbon balance under varying temperature and moisture regimes *J. Geophys. Res.* **115** G00I02
Jia G J *et al* 2002 Spatial characteristics of AVHRR-NDVI along latitudinal transectsin northern Alaska *J Veg. Sci.* **13** 315–26
Jia G J *et al* 2004 Controls over intra-seasonal dynamics of AVHRR NDVI for the Arctic tundra in northern Alaska *Int. J. Remote Sens.* **25** 1547–64
McGuire A D 2003 Arctic Transitions in the Land–Atmosphere System (ATLAS): background, objectives, results, and future directions *J. Geophys. Res.* **108** 8166
Muller S V *et al* 1999 Landsat MSS-derived land-cover map of northern Alaska: extrapolation methods and a comparison with photo-interpreted and AVHRR-derived maps *Int. J. Remote Sens.* **20** 2921–46
Myers-Smith I H *et al* 2011 Shrub expansion in tundra ecosystems: dynamics, impacts and research priorities *Environ. Res. Lett.* **6** 045509
Raynolds M K *et al* 2012 A new estimate of tundra-biome phytomass from trans-Arctic field data and AVHRR NDVI *Remote Sens. Lett.* **3** 403–11
Raynolds M K *et al* 2006 NDVI patterns and phytomass distribution in the circumpolar Arctic *Remote Sens. Environ.* **102** 271–81
Riedel S *et al* 2005a Spatial and temporal heterogeneity of vegetation properties among four tundra plant communities at Ivotuk, Alaska U. S. A. *Arct. Antarctic Alpine. Res.* **37** 25–33
Riedel S M *et al* 2005b Biotic controls over spectral reflectance of arctic tundra vegetation *Int. J. Remote Sens.* **26** 2391–405
Serreze M C and Francis J A 2006 The arctic amplification debate *Climatic Change* **76** 241–64
Silapaswan C *et al* 2001 Land cover change on the Seward Peninsula: the use of remote sensing to evaluate the potential influences of climate warming on historical vegetation dynamics *Can. J. Remote Sens.* **27** 542–54
Stow D A *et al* 2004 Remote sensing of vegetation and land-cover change in Arctic Tundra Ecosystems *Remote Sens. Environ.* **89** 281–308
Sturm M *et al* 2001 Snow-shrub interactions in Arctic Tundra: a hypothesis with climate implications *J. Clim.* **14** 336–44
Sturm M *et al* 2005 Winter biological processes could help convert Arctic tundra to shrubland *BioScience* **55** 17–26
Tenhunen J D *et al* 1992 The ecosystem role of poikilohydric tundra plants *Arctic Ecosystems in a Changing Climate: An Ecosphysiological Perspective* ed F S III Chapin *et al* (San Diego, CA: Academic) pp 213–39
Tibshirani R 1996 Regression shrinkage and selection via the lasso *J. Roy. Stat. Soc. B Met.* **58** 267–88
Ueyama M *et al* 2013 Growing season and spatial variations of carbon fluxes of Arctic and boreal ecosystems in Alaska (USA) *Ecol. Appl.* **23** 1798–816
Ustin S L and Gamon J A 2010 Remote sensing of plant functional types *New Phytol.* **186** 795–816
van der Wal R and Stien A 2014 High arctic plants like it hot: a long-term investigation of between-year variability in plant biomass *Ecol. Soc. Am.* **95** 3414–27
Walker D *et al* 1995 NDVI, biomass, and landscape evolution of glaciated terrain in northern Alaska *Polar Rec.* **31** 169–78
Walker D *et al* 2005 The Circumpolar Arctic vegetation map *J. Veg. Sci.* **16** 267–82
Walker D A 1999 An integrated vegetation mapping approach for northern Alaska (1:4 M scale) *Int. J. Remote Sens.* **20** 2895–920
Walker D A 2003 Phytomass, LAI, and NDVI in northern Alaska: relationships to summer warmth, soil pH, plant functional types, and extrapolation to the circumpolar Arctic *J. Geophys. Res.* **108** 8169
Walker D A *et al* 2003 Vegetation-soil-thaw-depth relationships along a low-arctic bioclimate gradient, Alaska: synthesis of information from the ATLAS studies *Permafrost Periglac.* **14** 103–23
Walker D A *et al* 2012 Environment, vegetation and greenness (NDVI) along the North America and Eurasia Arctic transects *Environ. Res. Lett.* **7** 015504
Walker M D *et al* 1994 Plant communities of a tussock tundra landscape in the Brooks Range Foothills, Alaska *J. Veg. Sci.* **5** 843–66
Walker M D *et al* 2006 Plant community responses to experimental warming across the tundra biome *Proc. Natl Acad. Sci. USA* **103** 1342–6
Westhoff V and van der Meel E 1973 The Braun-Blanquet approach *Ordination and Classification of Communities* ed R H Whittaker (Den Haag, NL: Dr. W. Junk) pp 617–726
Winton M 2006 Amplified Arctic climate change: What does surface albedo feedback have to do with it? *Geophys. Res. Lett.* **33** L03701
Xu H *et al* 2014 Evaluating remotely sensed phenological metrics in a dynamic dcosystem model *Remote Sens.* **6** 4660–86
Zeng H *et al* 2011 Recent changes in phenology over the northern high latitudes detected from multi-satellite data *Environ. Res. Lett.* **6** 045508